DOI: 10.1002/zaac.200900019

Chemical Hardness and the Adaptive Coordination Behavior of the d^0 Transition Metal Oxide Fluoride Anions

Michael R. Marvel,[a] Rachelle Ann F. Pinlac,[b] Julien Lesage,[b] Charlotte L. Stern,[b] and Kenneth R. Poeppelmeier*[b]

Dedicated to Professor Gerd Meyer on the Occasion of His 60th Birthday

Keywords: Hydrothermal synthesis; X-ray diffraction; Oxyfluorides; Bond valence

Abstract. Five new isostructural d^0 transition metal oxide fluoride compounds $Rb_3Na(NbOF_5)_2 \cdot H_2O$ and $A_3Na(MO_2F_4)_2 \cdot H_2O$ (A = K, Rb and M = Mo, W) have been synthesized by hydrothermal methods and their original structures determined by single-crystal X-ray diffraction. In these compounds, the sodium ions preferentially engage in strong electrostatic interactions with the least polarizable fluoride ions and concurrently the Nb^{5+}, M^{6+} (M = Mo, W) metal centers displace toward the oxide ion(s) located *trans* to the fluorides in order to maintain atomic valences. Consequently, the oxide and fluoride sites retain unequal charge and the most negatively charged ions form the most/strongest interactions with the cations. The electrostatic potentials and the chemical hardness differences of the oxide and fluoride ions thus determine the anion connectivities: the *cis*-oxo $MO_2F_4^{2-}$ anions (M = Mo, W) engage in the most/strongest electrostatic interactions with the alkali counter-cations through the two fluorides *trans* to the *cis* oxides. The $NbOF_5^{2-}$ anion forms its most/strongest electrostatic interactions with the cations through the one fluoride position *trans* to the oxide.

Introduction

Structural building units which show an inherent dipole moment are attractive because they can potentially lead to interesting properties if they are aligned in a non-centrosymmetric manner. In that respect, the factors that determine the three-dimensional bond networks and can lead to non-centrosymmetric crystal packing of the $NbOF_5^{2-}$ and $MO_2F_4^{2-}$ (M = Mo, W) anions in inorganic-organic hybrids have been studied thoroughly [1−4]. The early d^0 transition metals in the $NbOF_5^{2-}$ and $MO_2F_4^{2-}$ (M = Mo, W) anions undergo primary electronic distortions owing to metal dπ−oxygen pπ orbital interactions and move accordingly from the center of the octahedra toward one of its corner or edge, respectively. As a result, the oxide and fluoride ions retain unequal amounts of residual negative charge and impacts the way they coordinate to the surrounding cations. See Figure 1.

For example, in $[pyridineH]_2[Cu(pyridine)_4NbOF_5]$ [1], $Cd(3\text{-aminopyridine})_4NbOF_5$ [4] and $Cd(pyridine)_4NbOF_5$ [5], the $NbOF_5^{2-}$ anion coordinates through the oxide ion and *trans*-fluoride, and is a *trans*-director. Similarly, in $[HNC_6H_6OH]_2[Cu(NC_5H_5)_4(WO_2F_4)_2]$ [3], the *cis*-oxo $WO_2F_4^{2-}$ anion bonds to the copper cation and the HN group through one oxide ion and the fluoride ion *trans* to it, and perhaps surprisingly, is also a *trans*-director. An additional third contact is made by the other *trans*-fluoride ion to the hydrogen atom of the hydroxo group. In contrast, the *cis-oxo* $[MoO_2F_4]^{2-}$ anion behaves as a *cis*-director, as in $M(pyz)_2(H_2O)_2MoO_2F_4$ (M = Zn, Cd) [1, 6].

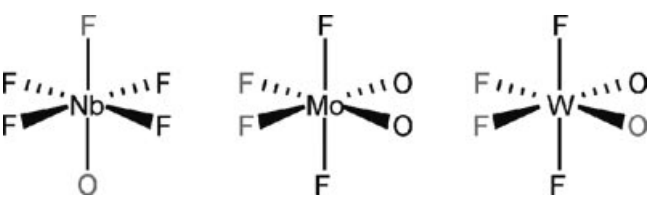

Figure 1. The $NbOF_5^{2-}$, $MoO_2F_4^{2-}$ and $WO_2F_4^{2-}$ anions. The O/F anionic ligands that retain the most residual negative charge following the out-of-center transition-metal distortions are shown in grey.

The factors that determine the connectivities of the $[MO_xF_{6-x}]^{n-}$ anions in completely inorganic solids are not well known because the anions typically crystallize with the

* Prof. Dr. K. R. Poeppelmeier
Fax: +1-847-491-7713
E-Mail: krp@northwestern.edu
[a] Department of Chemistry
Aurora University
347 S. Gladstone Ave.
Aurora, IL 60506, USA
[b] Department of Chemistry
Northwestern University
2145 Sheridan Road
Evanston, IL 60208−3113, USA

Supporting information for this article is available on the WWW under **www.zaac.wiley-vch.de** or from the author.

oxide and fluoride ions disordered, preventing bond-valence analysis. A recent examination of the cation−anion interactions in $KNaNbOF_5$ and $CsNaNbOF_5$, the first reported examples of an ordered $[NbOF_5]^{2-}$ anion in an inorganic phase, revealed topological connectivities determined by electronic potentials and chemical hardness [7].

Examination of the cation-anion interactions in the isostructural mixed-cation phases $Rb_3Na(NbOF_5)_2 \cdot H_2O$, $K_3Na(MoO_2F_4)_2 \cdot H_2O$, $Rb_3Na(MoO_2F_4)_2 \cdot H_2O$, $K_3Na(WO_2F_4)_2 \cdot H_2O$ and $Rb_3Na(WO_2F_4)_2 \cdot H_2O$ indicates that electronic potentials and chemical hardness also determine the connectivities of the anionic units. In particular, the $[WO_2F_4]^{2-}$ anions in $A_3Na(WO_2F_4)_2 \cdot H_2O$ (A = K, Rb) coordinate more strongly to the surrounding cations through the two fluorides *trans* to the oxides and is a *cis*-director for the first time. The adaptive coordination behavior of these anions renders them attractive building units and suggests that their long-range assembly may be controlled by careful selection of counter-cations.

Experimental Section

Synthesis

Caution: Hydrofluoric acid is toxic and corrosive, and must be handled with extreme caution and the appropriate protective gear! If contact with the liquid or vapor occurs, proper treatment procedures should immediately be followed [8].

Materials: Nb_2O_5 (99.9 %, Aldrich), $Na_2WO_4 \cdot 2H_2O$ (99.9 %, Aldrich), $Na_2MoO_4 \cdot 2H_2O$ (99.9 %, Aldrich), NaF (99.9 %, Aldrich), KF (99.9 %, Aldrich), RbF (99.9 %, Aldrich) and aqueous hydrofluoric acid (HF) (48 % HF by weight, Aldrich) were used as received. Owing to their hygroscopic nature, the alkali fluorides were manipulated under nitrogen in a dry box.

General Procedure: All reactants were sealed in Teflon [fluoro-(ethylenepropylene)] "pouches" [9]. Single or multiple pouches were placed in a Parr pressure vessel filled 33 % with deionized H_2O as backfill [10]. The pressure vessel was heated for 24 h at 150 °C and cooled to room temperature over an additional 24 h. The pouches were opened in air, and the products were recovered by vacuum filtration. In all reactions, excess solvent water or 48 % $HF_{(aq.)}$ was added and the A:Na:M (A = K, Rb; M = Nb, Mo, W) ratio of starting materials was kept at 1:2:1, except for $K_3Na(MoO_2F_4)_2 \cdot H_2O$. Reactions that deviated from this ratio by more than a factor of two led to the precipitation of secondary phases such as Rb_2NbOF_5 and Na_2NbOF_5 [11].

Na_2NbOF_5: Na_2NbOF_5 [11] was synthesized by reacting NaF (0.1344 g, 0.0032 mol), Nb_2O_5 (0.4253 g, 0.0016 mol), and 48 % aqueous HF (1.200 g, 0.0600 mol) for 24 h.

$Rb_3Na(NbOF_5)_2 \cdot H_2O$: $Rb_3Na(NbOF_5)_2 \cdot H_2O$ was synthesized by reacting RbF (0.0418 g, 0.0004 mol), Na_2NbOF_5 (0.1000 g, 0.0004 mol), and H_2O (1.000 g). Colorless needles were recovered in 40 % yield based on Nb. Attempts to synthesize $Rb_3Na(NbOF_5)_2 \cdot H_2O$ from Nb_2O_5, NaF, RbF, and 48 % aqueous HF led to the isolation of a mixed phase product of Na_2NbOF_5 [11] and $Rb_5Nb_3O_3F_{14} \cdot H_2O$ [12].

$K_3Na(WO_2F_4)_2 \cdot H_2O$: $K_3Na(WO_2F_4)_2 \cdot H_2O$ was synthesized by reacting KF (0.1755 g, 0.0030 mol), $Na_2WO_4 \cdot 2H_2O$ (1.000 g, 0.0030 mol), and 48 % aqueous HF (1.000 g, 0.0500 mol). Colorless needles were recovered in 57 % yield based on W.

$Rb_3Na(WO_2F_4)_2 \cdot H_2O$: $Rb_3Na(WO_2F_4)_2 \cdot H_2O$ was synthesized by reacting RbF (0.3166 g, 0.0030 mol), $Na_2WO_4 \cdot 2H_2O$ (1.000 g, 0.0030 mol), and 48 % aqueous HF (1.000 g, 0.0500 mol). Colorless needles were recovered in 55 % yield based on W.

$K_3Na(MoO_2F_4)_2 \cdot H_2O$: $K_3Na(MoO_2F_4)_2 \cdot H_2O$ was synthesized by reacting NaF (0.0729 g, 0.0017 mol), KF (0.2108 g, 0.0035 mol), MoO_3 (0.2500 g, 0.0017 mol), and 48 % aqueous HF (0.5000 g, 0.0250 mol). Colorless needles were recovered in 41 % yield based on Mo.

$Rb_3Na(MoO_2F_4)_2 \cdot H_2O$: $Rb_3Na(MoO_2F_4)_2 \cdot H_2O$ was synthesized by reacting RbF (0.4319 g, 0.0041 mol), $Na_2MoO_4 \cdot 2H_2O$ (1.000 g, 0.0041 mol), and 48 % aqueous HF (1.000 g, 0.0500 mol). Colorless needles were recovered in 60 % yield based on Mo.

Crystallographic Determination

Single-crystal X-ray diffraction data were collected with Mo-K_α radiation (λ = 0.71073 Å) with a Bruker-AXS SMART-1000 CCD diffractometer at 150 K (crystal **1**, **2**, **5** in Table 1) or a Bruker-AXS SMART APEX II diffractometer at 100 K (crystal **3**, **4** in Table 1) equipped with a graphite monochromator and using strategies based on ϕ and ω scans.

The data were then processed and integrated with the APEX II program suite [13]. The structures were solved by direct methods and successive Fourier difference synthesis and refined against F^2 by full-matrix least-squares techniques with SHELX [14]. A face-indexed absorption correction was performed numerically using the programs XPREP and the intensities were scaled with SADABS. All structures were checked for missing symmetry elements with PLATON [15]. The final refinement includes anisotropic displacement parameters and secondary extinction, when applicable. Further details of the crystal structure investigations may be obtained from Fachinformationszentrum Karlsruhe, 76344 Eggenstein-Leopoldshafen, Germany (Fax: +49-7247-808-666; E-Mail: crysdata(at)fiz-karlsruhe.de, http://www.fiz-karlsruhe.de/request_for_deposited_data.html) on quoting the 420281 (**1**), 420284 (**2**), 420285 (**3**), 420282 (**4**), 420283 (**5**) CSD numbers. Crystallographic data for the five compounds are collected in Table 1 and their atomic parameters available in Supporting Information (Table S1 to S5).

Spectroscopic Measurement

Mid-Infrared (400−4000 cm^{-1}) spectrum was collected with a sample of $Rb_3Na(NbOF_5)_2 \cdot H_2O$ with a Bio-Rad FTS-60 FTIR spectrometer operating at a resolution of 2 cm^{-1}. The sample was ground and pelletized with dried KBr, transferred to the FTIR spectrometer and evacuated for 2 to 5 min before spectra acquisition.

Results and Discussion

Bond Valence Calculation

The atomic X-ray scattering factors of oxygen and fluorine are similar; therefore bond-lengths and bond-valence

Zeitschrift für anorganische und allgemeine Chemie ZAAC Journal of Inorganic and General Chemistry

Table 1. Crystallographic data for (**1**) $Rb_3Na(NbOF_5)_2 \cdot H_2O$, (**2**) $K_3Na(WO_2F_4) \cdot H_2O$ and (**3**) $Rb_3Na(WO_2F_4)_2 \cdot H_2O$, (**4**) $K_3Na(MoO_2F_4)_2 \cdot H_2O$, (**5**) $Rb_3Na(MoO_2F_4)_2 \cdot H_2O$.

Compound	**1**	**2**	**3**
Formula	$H_2F_{10}NaNb_2O_3Rb_3$	$H_2F_8K_3NaO_5W_2$	$H_2F_8NaO_5Rb_3W_2$
Formula weight /g·mol^{-1}	705.24	742.01	881.12
Crystal system	monoclinic	monoclinic	monoclinic
Space group	*C*2/*m*	*C*2/*m*	*C*2/*m*
a /Å	20.623(3)	20.167(2)	20.4518(7)
b /Å	6.0634(9)	5.9354(6)	6.0020(2)
c /Å	12.1060(19)	11.8186(13)	11.9927(4)
β /degree	123.225(2)	123.6030(10)	123.2570(10)
V /A^3	1266.3(3)	1178.3(2)	1231.02(7)
Z	4	4	4
Crystal size /mm	0.02 × 0.05 × 0.17	0.01 × 0.03 × 0.21	0.25 × 0.27 × 0.48
T /K	153(2)	153(2)	100(2)
λ /Å	0.71073	0.71073	0.71073
θ range /degree	2.01−26.35	2.07−26.73	2.38−47.76
Data completeness	1.000	0.999	0.998
Measured reflections	5188	4964	29658
Independent reflections	1421	1379	6172
$\rho_{calcd.}$ /g·cm^{-3}	3.699	4.183	4.754
μ /mm^{-1}	13.421	20.723	30.606
R(*F*)[a)]	0.0400	0.0205	0.0362
$wR_2(F^2)$[b)]	0.1151	0.0488	0.0998
Compound	**4**	**5**	
Formula	$H_2F_8K_3Mo_2NaO_5$	$H_2F_8Mo_2NaO_5Rb_3$	
Formula weight /g·mol^{-1}	566.19	705.3	
Crystal system	monoclinic	monoclinic	
Space group	*C*2/*m*	*C*2/*m*	
a /Å	20.2947(5)	20.818(3)	
b /Å	5.86650(10)	6.0076(8)	
c /Å	11.7062(3)	11.9818(16)	
β /degree	124.4160(10)	124.1900(10)	
V /A^3	1149.76(5)	1239.5(3)	
Z	4	4	
Crystal size /mm	0.46 × 0.33 × 0.29	0.08 × 0.12 × 0.13	
T /K	100(2)	153(2)	
λ /Å	0.71073	0.71073	
θ range /degree	2.11−44.16	2.05−27.09	
Data completeness	0.998	0.995	
Measured reflections	21084	5355	
Independent reflections	4825	1490	
$\rho_{calcd.}$ /g·cm^{-3}	3.271	3.779	
μ /mm^{-1}	3.424	13.874	
R(*F*)[a]	0.0287	0.0253	
$wR_2(F^2)$[b]	0.0757	0.0664	

a) $R = \Sigma||F_o| - |F_c||/\Sigma|F_o|$ with $I > 2\,\sigma(I)$. b) $wR_2 = [\Sigma w(F_o^2 - F_c^2)^2/\Sigma w(F_o^2)^2]^{1/2}$.

relationships are used to determine the assignment and partial negative charges of each ligand around the transition-metal atoms. Owing to the small number of fluoride structures currently known, the bond lengths available to perform the calculation described by *Brown* [16] does not form a sufficient data set to retrieve reliable parameters for the given bond valence exponential relationship. However, in such cases, *Brese and O'Keeffe* proposed useful extrapolated parameters [17].

Analysis of well-characterized oxyfluorides structures obtained recently [2, 4, 5, 7, 18] shows systematically strong overbonding around niobium atoms. Therefore, in order to achieve a bond valence sum as close as possible to the expected value of five for niobium in $NbOF_5$ anions, calculations based on this new dataset have been performed. We calculate a value of $R_0 = 1.829$ Å for Nb−F bond (instead of 1.87 Å from the extrapolated value [17]), with the universal constant $B = 0.37$ and the value given by *Brown* [16] for Nb−O. Too few well-characterized anions are known to perform the same procedure for Mo−F and W−F bonds but the extrapolated values given by *Brese* and *O'Keeffe* appear suitable [17]. Finally, a new value of R_0 for the Rb−F bond is used in this work instead of 2.16 Å, the only available extrapolated value. Following the method described by *Brown* [16] on a dataset of 64 bonds in 56 well-characterized fluorides deposited in the ISCD (version 2008−2) [19], the value 2.106 Å with the universal *B* constant is proposed (standard deviation of 0.182 Å).

Infrared Study and Description of the Water Molecule

Infrared spectrum of $Rb_3Na(NbOF_5)_2 \cdot H_2O$ shows slightly doubled vibration bands at 920 cm^{-1}, which correspond to the two independent Nb=O bonds in the structure, whereas the equatorial Nb−F bonds show a broad band at 515 cm^{-1}. The broad peak between 3450−3650 cm^{-1} and the in-plane bending band at 1620 cm^{-1} are characteristic of water in the solid state. Free refinement of the occupation of the water molecule in all structures converges to 0.55(2) instead of 0.5, while it converges to 0.4(2) if the oxide atom is replaced by a fluorine atom. Attempts to refine mixed occupancy of H_2O and HF, their sum being constrained to 0.5 did not converge. Based on this analysis and the infrared study, we can assume that the proposed formula with water as the neutral coordinate is correct. Moreover, HF molecule has never been described as a suitable coordination molecule, whereas alkali hydrates are numerous and well described [20]. However, the positions of the hydrogen atoms of the water molecule were not determined. The water molecule coordinates tetrahedrally to a sodium and rubidium cation and two of three possible oxide and/or fluoride anions; the displacement parameters of the atoms involved show values about twice others. Some residual electron density is also observed in $K_3Na(MoO_2F_4)_2 \cdot H_2O$ between the water molecule and the coordinating sodium cation. Those observations show that the water molecule likely adopts several different hydrogen bonding schemes.

Structure Description

The framework of the $Rb_3Na(NbOF_5)_2 \cdot H_2O$ structure is shown in Figure 2; $A_3Na(MO_2F_4)_2 \cdot H_2O$ (A = K, Rb and M = Mo, W) structures have the same extended bond network. Three independent A cations (A = K, Rb) are twelve-coordinate with oxygen, fluoride and H_2O ligands whereas two crystallographic distinct sodium and niobium or M transition-metal cations are six-coordinate. It should be noted that, throughout the following discussion, M atoms correspond to either molybdenum or tungsten atoms. The same atom numbering is used to describe the five structures and facilitate comparisons. The description of eventual disorder of the anionic ligand in the structure on each crystallographic site is ensured by a chronological numbering which does not distinguish between oxide and fluoride atoms. The various X sites can therefore be occupied either by oxygen or fluoride depending on the structure considered. The sites $X1$ through $X4$ (X = O, F) are bonded to the first Nb1 or $M1$ atoms and the sites $X5$ to $X8$ are bonded to the second Nb2 or $M2$ atoms. The water molecule is labeled O9w.

The framework of the title compounds can be described as the stacking of layers along the a axis (Figure 2). The projection of a single layer along [101] shows that it is formed by the connection of two independent ribbons running along the b axis (Figure 3). $Na1F_6$ octahedra share the corners of one plane with four $Nb1OF_5$ or $M1O_2F_4$ octahedra to form the first type of infinite ribbons where two M octahedra alternate with one sodium octahedron. Another similar but independent type of infinite ribbons is built by the junction of two $Nb2OF_5$ or $Mo2O_2F_4$ and one $Na2F_4(H_2O)_2$ for the niobium and molybdenum structures in one hand, and $W2O_2F_4$ and either $Na2F_4(H_2O)_2$ or $Na2O_2F_2(H_2O)_2$ for the tungsten structures in the other. The Na1 octahedra in the first ribbon are linked to the Nb2 or $M2$ octahedra in the second ribbon through the apical

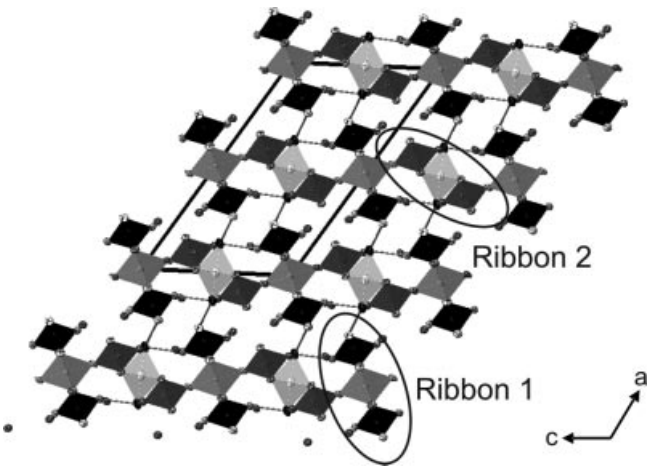

Figure 2. Projection of the $Rb_3Na(NbOF_5)_2 \cdot H_2O$ structure along the b axis. Ribbon 1 is built from one $Na1F_6$ (medium gray) and two $Nb1OF_5$ (black) octahedra. Ribbon 2 contains one $Na2F_4(H_2O)_2$ (light gray) and two $Nb2OF_5$ (dark gray) octahedra. The ellipsoids represent Rb^+ cations and the bonds correspond to potential hydrogen bonds between the water molecules and either an oxide, fluoride, or mixed ligands. $A_3Na(MO_2F_4)_2 \cdot H_2O$ (A = K, Rb; M = Mo, W) structures exhibit the same extended bond network.

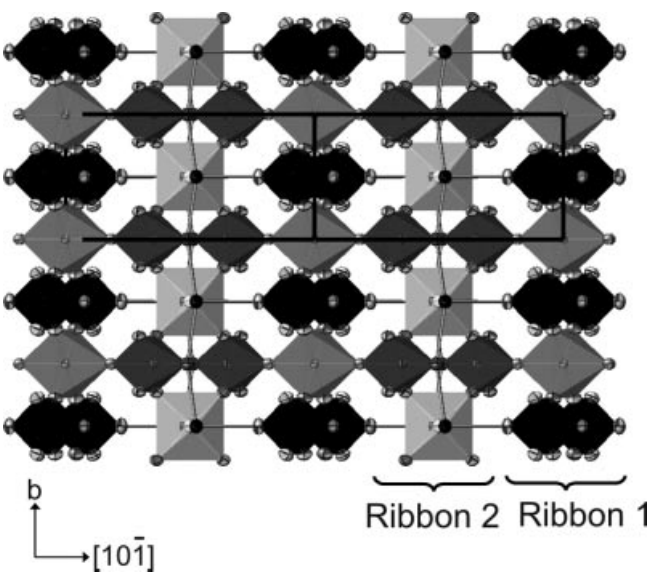

Figure 3. Projection along [101] of a single layer of the $Rb_3Na(NbOF_5)_2 \cdot H_2O$ structure where the two infinite ribbons along the b axis are indicated. See Figure 2 for complete legend.

Zeitschrift für anorganische und allgemeine Chemie ZAAC Journal of Inorganic and General Chemistry

fluoride ligand F6 *trans* to the O5 oxide ligand of the transition-metal anion along the *c* axis, forming infinite layers in the (*b*,*c*) plane.

Potential hydrogen bonds can be expected between the water molecule of Na2 octahedron and the O5 oxide ligand in the same ribbon along the *b* axis and the F3 fluoride ligands with the adjacent ribbon along the *c* axis (Figure 3). The layers are stacked along the *a* axis through the *A* cation (*A* = K, Rb) and other potential hydrogen bonds between the water molecule and the O1 site (in the molybdenum and tungsten cases) or either O1 and F1 sites (in the niobium case) along the *a* axis (Figure 2).

Disorder Models

Careful examination of the atomic displacement parameters of the two transition-metal sites shows that one of them is quasi-isotropic with small values consistent with the small size of such cations, as seen on Figure 4 c, 5 a and 6 a. In contrast, the other exhibits larger ellipsoids elongated along one direction in the niobium and molybdenum cases (Figure 4 a and 6 b) or two directions in the tungsten cases (Figure 5 b) toward the anionic ligands. This phenomenon results from the partial orientational statistic disorder of one of the two transition-metal sites. It is important to note that Nb1 shows orientational disorder in $Rb_3Na(NbOF_5)_2\cdot H_2O$ while *M*2 does in $Rb_3Na(MO_2F_4)_2\cdot H_2O$. In order to accurately describe the bonding scheme of the structures and calculate bond valences, the structures were refined in order to split the average position of the transition metal atoms in the "disordered" anion into discrete quasi-isotropical atomic positions. Note that if such refinements improve the structure model greatly, it improves the residual values only marginally.

$Rb_3Na(NbOF_5)_2\cdot H_2O$: The Nb1 atom is allowed to move outside of the mirror plane *m* and two discrete sites are refined with half occupancy. The *X*1 site is then refined with mixed O/F occupancy at a 0.5 ratio, their position and atomic displacement parameters being restrained to be the same. The distance between the two statistical niobium sites is 0.26(2) Å (Figure 4 b). Partial disorder resulting in an apparent edge-type distortion and similar Nb−Nb distance have been described previously in Na_2NbOF_5 [11]. As shown in Table 2, the short bond of 1.728(5) Å between Nb2 and *X*5 anion position indicates that it is occupied by an oxide ion. The long bond of 2.153(4) Å *trans* to the oxide ion is assigned to a fluoride ion (F6). The equatorial Nb2−F7 and Nb2−F8 distances have intermediate values 1.960(3) Å and 1.942(3) Å, respectively.

Despite its statistical orientational disorder, each discrete $Nb1OF_5^{2-}$ anion shows locally similar bond lengths: one short Nb1−O1 [1.733(8) Å] and one long Nb1−F2 bond [2.130(8) Å] *trans* to the Nb1−O1 bond. The remaining fluorides F1, F2, F3 and F4 are at intermediate distances of 1.928(9), 1.960(7), 1.937(4) and 1.925(4) Å from Nb1, respectively.

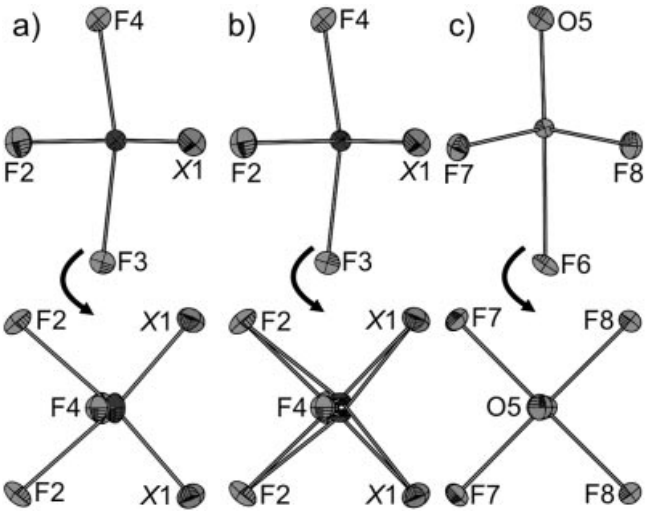

Figure 4. Thermal ellipsoid plots of (a) partially ordered Nb1-centered anions, (b) partially ordered Nb1 split into two positions and (c) ordered Nb2-centered anions in $Rb_3Na(NbOF_5)_2\cdot H_2O$. The top and bottom images are projections along the two perpendicular directions *b* and [30−8]. *X*1 has a 50:50 probability of containing oxide or fluoride.

Table 2. Selected bond lengths, bond valence calculations and environment of the ligands of the $NbOF_5^{2-}$ anions in $Rb_3Na(NbOF_5)_2\cdot H_2O$.

i−*j*	d_{ij} [a]	S_{ij} [b]	NC[c]	PC[d]	#N[e] Rb	Na	d_{jw} [f]
Nb1−O1	1.733(8)	1.62	0.38	0.30	3		2.960(6)
Nb1−F1	1.928(9)	0.77	0.23	0.19	3		2.960(6)
Nb1−F2	1.960(7)	0.70	0.30	0.40	4	1	
Nb1−F2	2.130(8)	0.44	0.56	0.40	4	1	
Nb1−F3	1.937(4)	0.75	0.25	0.25	3		3.055(8)
Nb1−F4	1.925(4)	0.77	0.23	0.24	3		
Nb2−O5	1.728(5)	1.64	0.36	0.16	1		2 × 3.0666(13)
Nb2−F6	2.153(4)	0.42	0.58	0.44	4	1	
Nb2−F7	1.960(3)	0.70	0.30	0.37	2	1	
Nb2−F7	1.960(3)	0.70	0.30	0.37	2	1	
Nb2−F8	1.942(3)	0.74	0.26	0.37	3		
Nb2−F8	1.942(3)	0.74	0.26	0.37	3		

a) Length in Å of the bond from the metal center cation *i* to the anionic ligand *j*. b) $S_{ij} = \exp[(R_0 - d_{ij})/B]$ in valence unit v. u. is the experimental bond valence or apparent valence AV, with R_0(Nb−O) = 1.911, R_0(Nb−F) = 1.829 and B = 0.37. c) NC = $z_j - S_{ij}$ in v. u. is the residual negative charge on the ligand *j*, with z_j its formal valence. d) PC = $\sum_{i'} S_{ji'}$ in v. u. is the positive charge surrounding ligand *j*, with $S_{ji'}$ the AV of bonds from the ligand *j* to the surrounding alkali cations *i*′ [R_0(Na−O) = 1.803, R_0(Na−F) = 1.677; R_0(Rb−O) = 2.263, R_0(Rb−F) = 2.106, see Table S6 for details]. e) Number of alkali cations surrounding the ligand *j*. f) Length in Å of the bond(s) from the ligand *j* to O9w atom of the surrounding water molecule(s) *w*.

$A_3Na(WO_2F_4)_2\cdot H_2O$ (A = K, Rb): The same refinement procedure is applied and converges for the tungsten structures. However, the anisotropic ellipsoids of the two generated positions equivalent by symmetry are elongated in the direction perpendicular to the mirror, indicating that these two positions should be further split in two, and their occu-

pation parameter accordingly divided by two. In order to model that disorder and obtain quasi-isotropical displacement ellipsoids, restraints are introduced into the model to prevent the four generated positions to come closer than about 0.2 Å from each other. Free refinement of the occupancy ratio of the two independent sites, the sum of them being restrained to 0.5, confirms that none of the two positions is predominant. The occupancies of each W2a and W2b atomic sites is then fixed at 0.25 and the occupation of their equatorial ligands *X*7 and *X*8 are fixed at a quarter of one oxide atom and three quarters of one fluorine atom, the atomic positions and displacement parameters of each site being restrained to be the same. This partial ordering in the long range of the $W2O_2F_4$ anion resulting in a corner-type distortion similar to the $Nb2OF_5$ anion (Figure 5 b and 4 c, respectively), has been observed on one previous occasion in $[pyH]_2[Cu(py)_4(WO_2F_4)_2]$ [6], where one W=O bond is ordered and the other oxide ion and three fluoride ions are disordered 1/4 and 3/4 over the equatorial ligand sites, in accordance with the stoichiometry. The distances W2a−W2a and W2b−W2b are 0.22(5) and 0.22(6) Å for the potassium compound and 0.197(8) and 0.183(11) Å for the rubidium compound (Figure 5 c). Note that an equivalent disorder model over four equivalent positions has been recently described in $(NH_4)_2WO_2F_4$ [21] with similar distances between the different positions. All of the crystallographic sites surrounding the W1 atom could be identified as oxide or fluoride ions. In $K_3Na(WO_2F_4)_2\cdot H_2O$, two short W1−O1 bonds [1.728(4) Å] *trans* to two long W1−F2 bonds [2.050(3) Å] are observed along with intermediate W1−F3 [1.920(4) Å] and W1−F4 [1.910(4) Å] bonds (Table 3).

Table 3. Selected bond lengths, bond valence calculations and environment of the ligands of the $WO_2F_4^{2-}$ anions in $K_3Na(WO_2F_4)_2\cdot H_2O$.

i−*j*	d_{ij} [a]	S_{ij} [b]	NC [c]	PC [d]	#N [e] K	#N [e] Na	d_{jw} [f]
W1−O1	1.728(4)	1.67	0.33	0.25	3		2.886(6)
W1−O1	1.728(4)	1.67	0.33	0.25	3		2.886(6)
W1−F2	2.050(3)	0.55	0.45	0.41	4	1	
W1−F2	2.050(3)	0.55	0.45	0.41	4	1	
W1−F3	1.920(4)	0.78	0.22	0.23	3		2.976(6)
W1−F4	1.910(4)	0.80	0.20	0.23	3		
W2a−O5	1.724(13)	1.69	0.31	0.15	1		2 × 3.0051(11)
W2a−F6	2.101(13)	0.48	0.52	0.44	4	1	
W2a−F7	1.912(18)	0.80	0.20	0.36	2	1	
W2a−F7	2.064(19)	0.53	0.47	0.36	2	1	
W2a−F8	1.91(2)	0.81	0.19	0.35	3		
W2a−O8	1.742(19)	1.60	0.40	0.51	3		
W2b−O5	1.732(13)	1.65	0.35	0.15	1		2 × 3.0051(11)
W2b−F6	2.087(13)	0.50	0.50	0.44	4	1	
W2b−F7	1.91(2)	0.81	0.19	0.36	2	1	
W2b−O7	1.75(2)	1.57	0.43	0.52	2	1	
W2b−F8	1.900(19)	0.83	0.17	0.35	3		
W2b−F8	2.05(2)	0.55	0.45	0.35	3		

a) Length in Å of the bond from the metal center cation *i* to the anionic ligand *j*. b) $S_{ij} = \exp[(R_0 - d_{ij})/B]$ in valence unit v. u. is the experimental bond valence or apparent valence AV, with $R_0(W-O) = 1.917$, $R_0(W-F) = 1.83$ and $B = 0.37$. c) $NC = z_j - S_{ij}$ in v. u. is the residual negative charge on the ligand *j*, with z_j its formal valence. d) $PC = \sum_{i'} S_{ji'}$ in v. u. is the positive charge surrounding ligand *j*, with $S_{ji'}$ the AV of bonds from the ligand *j* to the surrounding alkali cations *i*′ [$R_0(Na-O) = 1.803$, $R_0(Na-F) = 1.677$; $R_0(K-O) = 2.132$, $R_0(K-F) = 1.992$, see Table S7 for details]. e) Number of alkali cations surrounding the ligand *j*. f) Length in Å of the bond(s) from the ligand *j* to O9w atom of the surrounding water molecule(s) *w*.

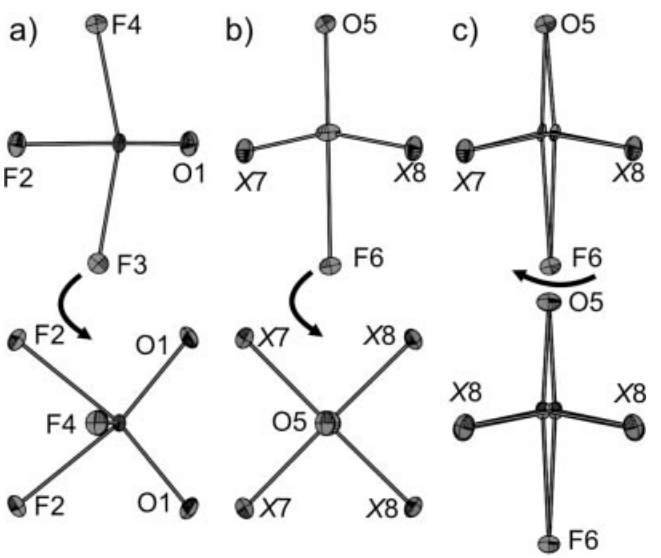

Figure 5. Thermal ellipsoid plots of (a) ordered W1-centered anions, (b) partially ordered W2-centered anions and (c) partially ordered W2 split into four positions in $Rb_3Na(WO_2F_4)_2\cdot H_2O$. The top and bottom images are projections along the two perpendicular directions: (a) and (b) *b* and [30−8], and (c) *b* and [203]. *X*7/*X*8 has a 25:75 probability of containing oxide or fluoride.

The local environment of W2 atoms observes similar pattern with two short distances [1.724(13) and 1.742(19) Å for W2a or 1.732(13) and 1.75(2) Å for W2b], two long distances [2.064(19) and 2.101(13) Å for W2a or 2.05(2) and 2.087(13) Å for W2b] and two intermediate distances [1.91(2) and 1.912(18) Å for W2a or 1.900(19) and 1.91(2) Å for W2b]. Similar bond lengths are observed in $Rb_3Na(WO_2F_4)_2\cdot H_2O$ (Table 4).

$A_3Na(MoO_2F_4)_2\cdot H_2O$ (A = K, Rb): For $K_3Na(MoO_2F_4)_2\cdot H_2O$, the same general refinement procedure was applied to the Mo2 site and two different sites were found at 0.208(3) Å from each other, as in $Rb_3Na(NbOF_5)_2\cdot H_2O$. The atom site *X*8 is occupied with half an oxide atom and half a fluorine atom with their atomic position and displacement parameters restrained to be the same (Figure 6 c), resulting in a face-type distortion (Figure 6 b). In $Rb_3Na(MoO_2F_4)_2\cdot H_2O$, the two discrete atomic sites observed still conserves anisotropy, as observed in the tungsten compounds. However, if the off-mirror Mo2 site is further split in two and the sum of their occupancies is constrained to 0.5, the occupancy of the atomic position pointing toward the *X*7 sites converge to 0.06(2). As a consequence, the MoO_2F_4 anionic units can scarcely adopt

Zeitschrift für anorganische und allgemeine Chemie ZAAC Journal of Inorganic and General Chemistry

Table 4. Selected bond lengths, bond valence calculations and environment of the ligands of the $WO_2F_4^{2-}$ anions in $Rb_3Na(WO_2F_4)_2 \cdot H_2O$.

$i-j$	d_{ij} [a]	S_{ij} [b]	NC [c]	PC [d]	#N [e] Rb	Na	d_{jw} [f]
W1−O1	1.731(2)	1.65	0.35	0.32	3		2.933(4)
W1−O1	1.731(2)	1.65	0.35	0.32	3		2.933(4)
W1−F2	2.0681(18)	0.53	0.47	0.43	4	1	
W1−F2	2.0681(18)	0.53	0.47	0.43	4	1	
W1−F3	1.923(3)	0.78	0.22	0.28	3		3.042(5)
W1−F4	1.906(3)	0.81	0.19	0.27	3		
W2a−O5	1.717(4)	1.72	0.28	0.16	1		2 × 3.0404(8)
W2a−F6	2.102(3)	0.48	0.52	0.46	4	1	
W2a−F7	1.907(4)	0.81	0.19	0.38	2	1	
W2a−F7	2.031(4)	0.58	0.42	0.38	2	1	
W2a−F8	1.895(5)	0.84	0.16	0.38	3		
W2a−O8	1.762(4)	1.52	0.48	0.57	3		
W2b−O5	1.707(4)	1.76	0.24	0.16	1		2 × 3.0404(8)
W2b−F6	2.111(3)	0.47	0.53	0.46	4	1	
W2b−F7	1.900(4)	0.83	0.17	0.38	2	1	
W2b−O7	1.756(3)	1.55	0.45	0.56	2	1	
W2b−F8	1.909(3)	0.81	0.19	0.38	3		
W2b−F8	2.040(3)	0.57	0.43	0.38	3		

a) Length in Å of the bond from the metal center cation i to the anionic ligand j. b) $S_{ij} = \exp[(R_0 - d_{ij})/B]$ in valence unit v. u. is the experimental bond valence or apparent valence AV, with R_0(Wb−O) = 1.917, R_0(Wb−F) = 1.83 and B = 0.37. c) NC = $z_j - S_{ij}$ in v. u. is the residual negative charge on the ligand j, with z_j its formal valence. d) PC = $\sum_{i'} S_{ji'}$ in v. u. is the positive charge surrounding ligand j, with $S_{ji'}$ the AV of bonds from the ligand j to the surrounding alkali cations i' [R_0(Na−O) = 1.803, R_0(Na−F) = 1.677; R_0(Rb−O) = 2.263, R_0(Rb−F) = 2.106, see Table S8 for details]. e) Number of alkali cations surrounding the ligand j. f) Length in Å of the bond(s) from the ligand j to O9w atom of the surrounding water molecule(s) w.

the other statistical orientation in that structure and the same model as $K_3Na(MoO_2F_4)_2 \cdot H_2O$ was applied to $Rb_3Na(MoO_2F_4)_2 \cdot H_2O$. The distance between the two molybdenum atoms generated by symmetry is nevertheless constrained to be no longer than about 0.2 Å and converges to 0.196(10) Å. The local Mo1 environment in $K_3Na(MoO_2F_4)_2 \cdot H_2O$ includes two *cis*-O positions (O1) with short distances [1.7058(13) Å] *trans* to two *cis*-F (F2) positions with long distances [2.0530(11) Å]. See Table 5. The two remaining F3 and F4 positions are located at intermediate distances of 1.9447(14) and 1.8936(15) Å, respectively. The Mo2 anion have locally similar environment with two short distances [1.6935(15) and 1.7501(15) Å], two long distances [2.0497(14) and 2.1035(13) Å] and two intermediate distances [1.9028(15) and 1.9107(15) Å]. Similar bond lengths are observed in $Rb_3Na(MoO_2F_4)_2 \cdot H_2O$ (Table 6). Finally, it is interesting to note that in the molybdenum structures, the F3 ion is the closest to the water molecule, in contrast to the niobium and tungsten structures where the O1 ion is the closest hydrogen-bond acceptor.

Chemical Hardness and Anion Connectivities

Electronic potentials and chemical hardness cooperatively influence the anions long-range order of the studied

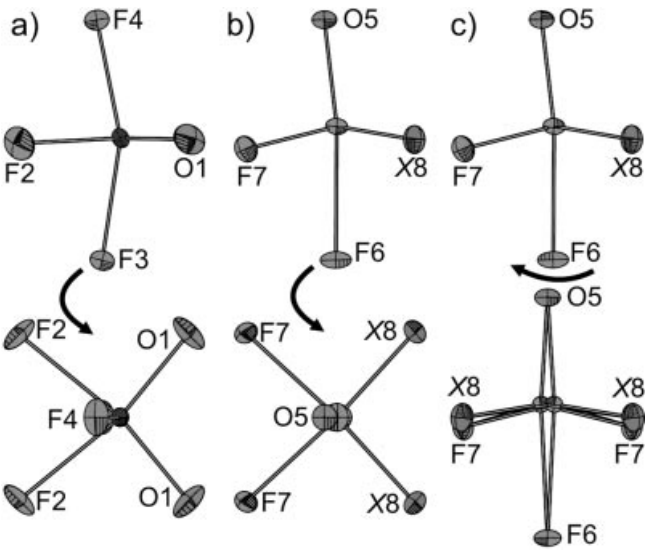

Figure 6. Thermal ellipsoid plots of (a) ordered Mo1-centered anions, (b) partially ordered Mo2-centered anions, and (c) partially ordered Mo2 split into two positions in $K_3Na(MoO_2F_4)_2 \cdot H_2O$. The top and bottom images are projections along two perpendicular directions: (a) and (b) b and [30−8], and (c) b and [203]. X8 has a 50:50 probability of containing oxide or fluoride.

Table 5. Selected bond lengths, bond valence calculations and environment of the ligands of the $MoO_2F_4^{2-}$ anions in $K_3Na(MoO_2F_4)_2 \cdot H_2O$.

$i-j$	d_{ij} [a]	S_{ij} [b]	NC [c]	PC [d]	#N [e] K	Na	d_{jw} [f]
Mo1−O1	1.7058(13)	1.72	0.28	0.23	3		2.903(2)
Mo1−O1	1.7059(13)	1.72	0.28	0.23	3		2.903(2)
Mo1−F2	2.0530(11)	0.52	0.48	0.44	4	1	
Mo1−F2	2.0529(11)	0.52	0.48	0.44	4	1	
Mo1−F3	1.9447(14)	0.69	0.31	0.24	3		2.784(3)
Mo1−F4	1.8936(15)	0.80	0.20	0.25	3		
Mo2−O5	1.6935(15)	1.78	0.22	0.12	1		2 × 2.9747(4)
Mo2−F6	2.1035(13)	0.45	0.55	0.49	4	1	
Mo2−F7	1.9107(13)	0.76	0.24	0.43	2	1	
Mo2−F7	2.0497(13)	0.52	0.48	0.43	2	1	
Mo2−F8	1.9028(15)	0.78	0.22	0.32	3		
Mo2−O8	1.7501(15)	1.53	0.47	0.46	3		

a) Length in Å of the bond from the metal center cation i to the anionic ligand j. b) $S_{ij} = \exp[(R_0 - d_{ij})/B]$ in valence unit v. u. is the experimental bond valence or apparent valence AV, with R_0(Mo−O) = 1.907, R_0(Mo−F) = 1.81 and B = 0.37. c) NC = $z_j - S_{ij}$ in v. u. is the residual negative charge on the ligand j, with z_j its formal valence. d) PC = $\sum_{i'} S_{ji'}$ in v. u. is the positive charge surrounding ligand j, with $S_{ji'}$ the AV of bonds from the ligand j to the surrounding alkali cations i' [R_0(Na−O) = 1.803, R_0(Na−F) = 1.677; R_0(K−O) = 2.132, R_0(K−F) = 1.992, see Table S9 for details]. e) Number of alkali cations surrounding the ligand j. f) Length in Å of the bond(s) from the ligand j to O9w atom of the surrounding water molecule(s) w.

compounds. Owing to the polarizability difference between the fluoride (0.81×10^{-24} cm^3) and oxide (3×10^{-24} cm^3) ions [22], the fluoride ions preferentially interact with the smaller Na^+ cations. For that reason, it is noteworthy that all inorganic solids composed of long-range ordered oxide

Table 6. Selected bond lengths, bond valence calculations and environment of the ligands of the $MoO_2F_4^{2-}$ anions in $Rb_3Na(MoO_2F_4)_2 \cdot H_2O$.

$i-j$	d_{ij} [a]	S_{ij} [b]	NC [c]	PC [d]	#N [e] Rb	Na	d_{jw} [f]
Mo1−O1	1.724(2)	1.64	0.36	0.29	3		2.993(4)
Mo1−O1	1.724(2)	1.64	0.36	0.29	3		2.993(4)
Mo1−F2	2.072(2)	0.49	0.51	0.44	4	1	
Mo1−F2	2.072(2)	0.49	0.51	0.44	4	1	
Mo1−F3	1.964(3)	0.66	0.34	0.27	3		2.828(5)
Mo1−F4	1.891(3)	0.80	0.20	0.27	3		
Mo2−O5	1.969(3)	1.77	0.23	0.13	1		2×2.0639(11)
Mo2−F6	2.121(3)	0.43	0.57	0.47	4	1	
Mo2−F7	1.899(4)	0.79	0.21	0.39	2	1	
Mo2−F7	2.032(4)	0.55	0.45	0.39	2	1	
Mo2−F8	1.923(4)	0.74	0.26	0.33	3		
Mo2−O8	1.781(4)	1.41	0.59	0.50	3		

a) Length in Å of the bond from the metal center cation i to the anionic ligand j. b) $S_{ij} = \exp[(R_0 - d_{ij})/B]$ in valence unit v. u. is the experimental bond valence or apparent valence AV, with R_0(Mo−O) = 1.907, R_0(Mo−F) = 1.81 and B = 0.37. c) NC = $z_j - S_{ij}$ in v. u. is the residual negative charge on the ligand j, with z_j its formal valence. d) PC = $\sum_{i'} S_{ji'}$ in v. u. is the positive charge surrounding ligand j, with $S_{ji'}$ the AV of bonds from the ligand j to the surrounding alkali cations i' [R_0(Na−O) = 1.803, R_0(Na−F) = 1.677; R_0(Rb−O) = 2.263, R_0(Rb−F) = 2.106, see Table S10 for details]. e) Number of alkali cations surrounding the ligand j. f) Length in Å of the bond(s) from the ligand j to O9w atom of the surrounding water molecule(s) w.

fluoride transition metal anions contain Na^+ cations. The strong affinity between Na^+ and F^- ions lead to a crystallographically observable distortion of the M metal center toward the oxide ions *trans* to the fluoride ions engaged in Na^+-F^- interactions. This behavior is clearly evident in the structures of the title compounds, where no oxide (except the water molecule on Na2) is bound to sodium sites. The $Na1F_6$ anion is of particular interest, for it connects the two independent transition metal anions through the F2 and F6 ligands. Those two ligands retain the most residual negative charge and are always crystallographically ordered on the long range in all the structures studied. The strong Na^+-F^- interactions reduce the amount of valence the F2 and F6 fluoride ions can give to their M metal centers. Consequently, the M−F2 and M−F6 bonds weaken and assume strong ionic character. To maintain their valence, the M atoms form shorter, more covalent bonds with the O1 and O5 oxides *trans* to the F2 and F6 fluorides.

The most negatively charged oxide and fluoride ions make the most/strongest contacts to the surrounding Na^+ and A^+ (A = K, Rb) cations and consequently direct toward the highest positive potentials. See Table 2 to Table 6. For example, in $Rb_3Na(NbOF_5)_2 \cdot H_2O$ (Table 2), the fluoride F6 *trans* to the oxide ion O5 retains the most residual negative charge (0.58 v. u.) and makes contact with four twelve-coordinate Rb^+ cations and one six-coordinate Na^+ cation; electrostatic interactions which together account for 0.44 v. u. of positive charge. The remaining fluoride ions, F7 and F8, retain less residual negative charges (0.30 v. u. and 0.26 v. u., respectively) and are three-coordinate, with a positive counterpart of 0.37 v. u. in both cases. The O5 oxide ion possesses 0.36 v. u. of residual negative charge and makes only one cationic contact with 0.16 v. u. of positive charge. In the partially ordered Nb1 anion, one F2 ion *trans* to the O1 oxide has a significantly higher residual negative charge of 0.56 v. u., but can coordinate to two equivalent higher positive counterparts of 0.40 v. u. That particular environment explains why the Nb1 anion is partially disordered, in contrast with the Nb2 anion where the environment corresponds to its expected type of distortion.

The "adaptive coordination" behavior of these anions is again shown by the M1 and M2 sites for molybdenum and tungsten. The ordered and disordered sites are reversed compared to the niobate. The environment of the $M1O_2F_4^{2-}$ anions in $A_3Na(MO_2F_4)_2 \cdot H_2O$ (A = K, Rb and M = Mo, W; Table 3 to Table 6) corresponds to their edge-type distortion and are completely ordered on the long range. For example, in the structure of $K_3Na(MoO_2F_4)_2 \cdot H_2O$, the *cis*-fluoride F2 sites coordinated to Mo1 retain 0.48 v. u. of residual negative charge and both are surrounded by five cations accounting for 0.44 v. u. of positive potential. The *cis*-oxide O1 *trans* to F2 and the apical F3 and F4 sites are three-coordinate and retain significantly less residual negative charge (0.28, 0.31 and 0.20 v. u., respectively) therefore they do not form similarly strong electrostatic interactions with the surrounding cations (positive counterparts of 0.23, 0.24 and 0.25 v. u., respectively). In the M2 anion, three ligands exhibit significantly higher residual negative charges whereas only two of them are surrounded by equivalent higher positive potentials. This configuration explains why that anion is only partially ordered, owing to the strong affinity between Na1 and F6 ions. Note that this anionic electronic configuration

Table 7. Selected bond lengths, bond valence calculations and environment of the ligands of the $WO_2F_4^{2-}$ anions in $[HNC_6H_6OH]_2[Cu(NC_5H_5)_4(WO_2F_4)_2]$ and $Na_2WO_2F_4$.

$i-j$	d_{ij} [a]	S_{ij} [b]	NC [c]	PC [d]	#N
$[HNC_6H_6OH]_2[Cu(NC_5H_5)_4(WO_2F_4)_2]$					
W−O1	1.772(2)	1.50	0.50		Cu
W−O2	1.714(2)	1.75	0.25		
W−F1	2.059(2)	0.54	0.46		NH
W−F2	2.029(2)	0.58	0.42		OH
W−F3	1.903(2)	0.82	0.18		
W−F4	1.908(2)	0.81	0.19		
$Na_2WO_2F_4$					
2×W−O	1.750(9)	1.57	0.43	0.36	2
2×W−F1	1.932(8)	0.77	0.23	0.33	2
2×W−F2	2.039(9)	0.58	0.42	0.43	2

a) Length in Å of the bond from the metal center cation i to the anionic ligand j. b) $S_{ij} = \exp[(R_0 - d_{ij})/B]$ in valence unit v. u. is the experimental bond valence or apparent valence AV, with R_0(W−O) = 1.917, R_0(W−F) = 1.83 and B = 0.37. c) NC = $z_j - S_{ij}$ in v. u. is the residual negative charge on the ligand j, with z_j its formal valence. d) PC = $\sum_{i'} S_{ji'}$ in v. u. is the positive charge surrounding ligand j, with $S_{ji'}$ the AV of bonds from the ligand j to the surrounding alkali cations i' [R_0(Na−O) = 1.803, R_0(Na−F) = 1.677].

Zeitschrift für anorganische und allgemeine Chemie ZAAC Journal of Inorganic and General Chemistry

(three higher negatively charge ligands) can be ordered in the presence of adequate cationic environment, as illustrated in $[HNC_6H_6OH]_2$-$[Cu(NC_5H_5)_4(WO_2F_4)_2]$ [3] (Table 7).

Similar preferential interaction phenomena were observed in the recently reported mixed cation niobium oxide fluorides, $KNaNbOF_5$ and $CsNaNbOF_5$, where the high fluoride:oxide ratios led to crystal frameworks in which the Na^+ cations are drawn into shorter, stronger electrostatic interactions than their larger counterparts (K^+, Cs^+) [7]. Bond valence sums showed that the Na^+ cations are significantly overbonded (1.20 vu) and the K^+ and Cs^+ cations are ideally bound (close to 1.0 vu).

Similarly, the fluoride ions in $Na_2WO_2F_4$ [23] have approximately equal or greater positive counterparts than the more negatively charged oxide ions (Table 7).

Only two compounds with ordered $WO_2F_4^{2-}$ anions have been reported prior to this work (see Table 7). The $WO_2F_4^{2-}$ anion found in $Na_2WO_2F_4$ [23] possesses *cis*-oxide ions that have 0.43 v. u. of residual negative charge *trans* to *cis*-fluoride ions that have 0.42 v. u. of residual negative charge. As a result, a pronounced coordination preference is not apparent. In contrast, the $WO_2F_4^{2-}$ anion found in $[HNC_6H_6OH]_2[Cu(NC_5H_5)_4(WO_2F_4)_2]$ [3] directs coordination in a *trans* fashion because one oxide ion and its *trans* fluoride retain more residual negative charge than the remaining oxide and fluoride ions. Finally, the $W1O_2F_4^{2-}$ anion found in $A_3Na(WO_2F_4)_2 \cdot H_2O$ (A = K, Rb) shows a preferential coordination to the *cis*-fluoride (F2) sites *trans* to the *cis*-oxide (O1) sites. While typical for the $MoO_2F_4^{2-}$ anion, this *cis*-directing property is observed for the first time for the $WO_2F_4^{2-}$ anion. It demonstrates the particular adaptive coordination behavior of that building unit.

Conclusions

Chemical hardness, directing properties of the oxyfluoride building units and the spatial configuration of their surrounding cationic environments are the three factors controlling long-range order in inorganic solids containing $NbOF_5^{2-}$ and $MO_2F_4^{2-}$ (M = Mo, W) anions with heterocationic bond networks. The strong affinity of sodium and fluoride ions suggests that long-range order of the building units is likely to be observed if the structure contains high relative ratio of those elements. Moreover, the directing properties of each anionic unit are well understood and interact strongly with the two aforementioned factors. Crystallographic ordering of the oxide and fluoride ligands occurs only if their negative charges correspond to strong equivalent cationic environments. In that respect, important progress in understanding and predicting the global connectivity of structures remains to be done if one wants to design non-centrosymmetric long-range d^0 transition metal oxyfluoride materials.

Supporting Information (see footnote on the first page of this article): Table of atomic coordinates, bond lengths, bond valence and bond valence sums for each structure, infrared spectrum of $Rb_3Na(NbOF_5)_2 \cdot H_2O$.

Acknowledgement

The authors gratefully acknowledge the support from the *National Science Foundation* (Solid State Chemistry Award No. DMR-0312136 and DMR-0604454) and the use of the Central Facilities supported by the MRSEC program of the *National Science Foundation* (DMR-0076097 and DMR-0520513) at the Materials Research Center of Northwestern University.

References

[1] K. R. Heier, A. J. Norquist, C. G. Wilson, C. L. Stern, K. R. Poeppelmeier, *Inorg. Chem.* **1998**, *37*, 76.
[2] M. E. Welk, A. J. Norquist, F. P. Arnold, C. L. Stern, K. R. Poeppelmeier, *Inorg. Chem.* **2002**, *41*, 5119.
[3] M. E. Welk, A. J. Norquist, C. L. Stern, K. R. Poeppelmeier, *Inorg. Chem.* **2001**, *40*, 5479.
[4] H. K. Izumi, J. E. Kirsch, C. L. Stern, K. R. Poeppelmeier, *Inorg. Chem.* **2005**, *44*, 884.
[5] P. C. R. Guillory, J. E. Kirsch, H. K. Izumi, C. L. Stern, K. R. Poeppelmeier, *Cryst. Growth Des.* **2006**, *6*, 382.
[6] K. R. Heier, A. J. Norquist, P. S. Halasyamani, A. Duarte, C. L. Stern, K. R. Poeppelmeier, *Inorg. Chem.* **1999**, *38*, 762.
[7] M. R. Marvel, J. Lesage, J. Baek, P. S. Halasyamani, C. L. Stern, K. R. Poeppelmeier, *J. Am. Chem. Soc.* **2007**, *129*, 13963.
[8] J. C. Bertolini, *J. Emerg. Med.* **1992**, *10*, 163; D. Peters, R. Miethchen, *J. Fluorine Chem.* **1996**, *79*, 161; E. B. Segal, *Chem. Health Saf.* **2000**, *7*, 18.
[9] W. T. A. Harrison, T. M. Nenoff, T. E. Gier, G. D. Stucky, *Inorg. Chem.* **1993**, *32*, 2437.
[10] A. J. Norquist, K. R. Heier, C. L. Stern, K. R. Poeppelmeier, *Inorg. Chem.* **1998**, *37*, 6495.
[11] R. Stomberg, *Acta Chim. Scand. A* **1984**, *38*, 603.
[12] T. A. Kaidalova, V. I. Pakhomov, E. S. Panin, *Koord. Khim.* **1976**, *2*, 554.
[13] Bruker APEX2 suite (SAINT v7.34A, XPREP v2008/2, SADABS v2008/1, *SHELXTL 6*.14), v2008.5−0; Bruker AXS, Inc.: Madison, WI, USA, **2008**.
[14] G. M. Sheldrick, *Acta Crystallogr., Sect. A* **2008**, *64*, 112.
[15] A. L. Spek *PLATON*, Utrecht University: Utrecht, The Netherlands, **2001**.
[16] I. D. Brown, D. Altermatt, *Acta Crystallogr., Sect. B* **1985**, *41*, 244.
[17] N. E. Brese, M. O'Keeffe, *Acta Crystallogr., Sect. B* **1991**, *47*, 192.
[18] A. J. Norquist, C. L. Stern, K. R. Poeppelmeier, *Inorg. Chem.* **1999**, *38*, 3448; P. Halasyamani, K. R. Heier, M. J. Willis, C. L. Stern, K. R. Poeppelmeier, *Z. Anorg. Allg. Chem.* **1996**, *622*, 479.
[19] G. Bergerhoff, I. D. Brown, in: *Crystallographic Databases*, H. Allen, (Ed.) IUCr: Chester, **1987**.
[20] G. Ferraris, M. Franchini-Angela, *Acta Crystallogr., Sect. B* **1972**, *28*, 3572.
[21] A. A. Udovenko, M. M. Laptash, *Acta Crystallogr., Sect. B* **2008**, *64*, 645.
[22] P. Hagenmuller, *Inorg. Solid Fluorides*, Academic Press, Inc., New York **1985**.
[23] M. Vlasse, J. M. Moutou, M. Cervera-Marzal, J. P. Chaminade, P. Hagenmuller, *Rev. Chim. Miner.* **1982**, *19*, 58.

Received: January 19, 2009
Published Online: April 8, 2009

